Systematics in pion double charge exchange

S. J. Greene,* W. J. Braithwaite, D. B. Holtkamp,† W. B. Cottingame,‡ and C. F. Moore
University of Texas at Austin, Austin, Texas, 78712

G. R. Burleson, G. S. Blanpied,§ A. J. Viescas,|| and G. H. Daw
New Mexico State University, Las Cruces, New Mexico, 88003

C. L. Morris and H. A. Thiessen
Los Alamos National Laboratory, Los Alamos, New Mexico, 87545
(Received 11 May 1981)

The initial results of a systematic investigation into pion-double-charge-exchange reactions are reported. Data consisting of angular distributions and excitation functions have been measured in an effort to determine the reaction mechanism and understand its implications for nuclear physics. Cross sections are presented for (π^+,π^-) reactions on ^{9}Be ^{12,13}C, ^{16,18}O, ^{24,26}Mg, ^{32}S, and ^{209}Bi. Surprising systematics of the reaction as functions of pion scattering angle and energy, as well as target mass and isospin, are revealed. The data are discussed in terms of two reaction models, one involving a higher-order optical potential and the other involving multiple reaction amplitudes.

NUCLEAR REACTIONS ^{9}Be, ^{12,13}C, ^{16,18}O, ^{24,26}Mg, ^{32}S, ^{209}Bi (π^+,π^-), $E=100-300$ MeV, $\theta=5°-33°$; measured $\sigma(E;\theta,A)$, double analog and nonanalog transitions; discuss second-order optical model, deduce two-amplitude model.

I. INTRODUCTION

The $(\pi^{\pm},\pi^{\mp})$ double-charge-exchange (DCX) reaction, long on the list of "exotic" nuclear reactions because of experimental difficulties, is an intriguing process. It has been discussed as a possible probe of two-nucleon correlations inside the nucleus,[1] and as a means of creating and studying nuclei far from the line of stability.[2]

Several facets of the reaction have engendered continuing theoretical interest. In lowest order, the reaction involves two nucleons and should then be sensitive to nucleon-nucleon correlations, as reflected, for example, in higher-order terms of the π-nucleus optical potential. Because it involves a double isospin flip of the projectile, the isospin structure of the nucleus should be strongly involved, which means that DCX is expected to show some sensitivity to the matter distribution. Since it should be possible with DCX to create proton-rich nuclear species, various mass formulas, and nuclear structure effects could be studied. Theoretical work has been especially productive in examining DCX with respect to the N-N correlations and higher-order optical potentials.[3-7] Figure 1 demonstrates the range of such pursuits prior to the measurement of constraining data.

DCX cross sections are generally less than 1 μb/sr and had thus remained practically inaccessible to researchers[8,9] before the advent of the meson facilities, LAMPF and SIN. Early LAMPF experiments[10] were the first to observe discrete, two-body final states in the (π^+,π^-) reaction. Transitions from targets with various isospins were observed, with the surprising result that nonanalog transitions from $T=0$ targets were found to be as strong as those analog transitions from $T=1$ targets. Transitions to the double-isobaric-analog state (DIAS) were expected to dominate because of the high degree of overlap between initial- and final-state wave functions. Data from SIN,[11] in conjunction with that from LAMPF, indicated that the cross section for ^{18}O$(\pi^+,\pi^-)^{18}$Ne (g.s.) might be strongly angle dependent.

Another LAMPF measurement[12] observed this strong angular dependence. At 164 MeV, the ^{18}O$(\pi^+,\pi^-)^{18}$Ne (DIAS) angular distribution showed an apparent diffractive shape, but with the

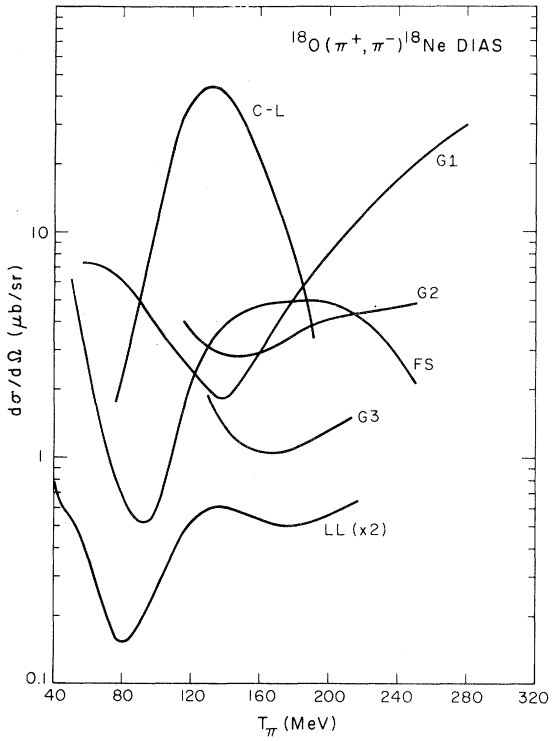

FIG. 1. Predictions of $^{18}O(\pi^+,\pi^-)^{18}Ne$ DIAS, forward-angle excitation functions, prior to the appearance of data. C-L, Chew-Low model of Ref. 3; *G*1, *G*2, and *G*3, Glauber calculations of Refs. 5, 28, and 30; FS, fixed scatterer of Ref. 4; and LL, local Laplacian of Ref. 6.

first minimum at a very small angle—nearly 20°. In standard elastic π-nucleus diffractive models this would imply an ^{18}O nuclear size of ~ 5.7 fm. This is unphysically large when compared with the electron scattering[13] and pion elastic scattering[14] value of ~ 3.8 fm.

These data were not sufficient to adequately appraise DCX as a probe for nuclear structure studies. A systematic investigation of the details and dependencies of the reaction was needed to elucidate the features of the reaction mechanism and its relation to nuclear structure.

We report here the initial results of such a program. DCX measurements have been performed which have given new information on the dependence of the process on angle, as well as on target mass and isospin. The utility of the technique for measuring new masses of proton-rich nuclei has been confirmed. The remainder of this paper is devoted to a presentation and discussion of this new data, and the current direction of analyses we are making.

II. EXPERIMENT

The EPICS pion spectrometer facility[15] at LAMPF was used for these experiments because of its high flux ($\sim 10^8$ π/s) and good resolution (~ 150 keV). A modification of the facility was designed by this collaboration to enable forward-angle DCX measurements.

With the EPICS sytem, high incident π^+ flux with good resolution is obtained through the momentum-dispersed beam technique; a $\Delta p/p = \pm 1\%$ of the central momentum is dispersed along 20 cm of target height. Incident momenta are determined by ray-tracing scattered particles back to the target, through a quadrupole triplet focusing element, from a set of delay-line readout multiwire drift chambers (F1-4) positioned at the front focus of the spectrometer dipoles as shown in Fig. 2. These chambers have a counting-rate limit of ~ 1 MHz. Forward of $\sim 18°$, however, the spectrometer intercepts a significant fraction of the unscattered beam, flooding the front chambers and degrading the resolution and live time. Yet, forward-angle DCX experiments require the highest available π^+ flux because of the very low cross sections.

In order to overcome these problems, a circular-dipole *C* magnet was used to magnetically separate the DCX π^- from the outgoing π^+ beam. Positioned immediately after the target, the magnet induced an opening angle of 20° between the oppositely charged pions. Sweeping away the π^+ beam reduced the front-chamber count rate sufficiently to allow measurement near 0°. This modification (inset Fig. 2) enabled negative pions of the selected scattering angle to enter and exit the field normal-

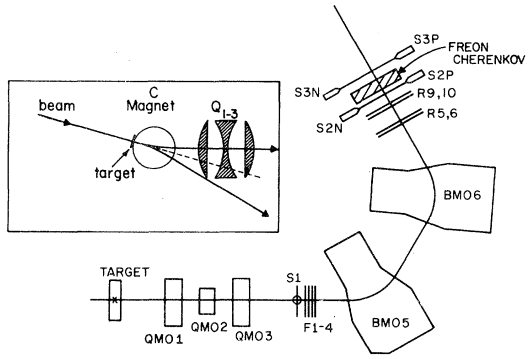

FIG. 2. Schematic elevation view of the EPICS spectrometer showing the detector positions. Inset: schematic plan view of the circular-magnet beam-sweeping modificiation to the EPICS spectrometer front end.

TABLE I. Targets, parameters, and differential cross sections for (π^+,π^-) at $5°_{lab}$ for 180 and 292 MeV.

Target	(mg/cm^2)	Chemical composition	Isotopic purity (%)	$d\sigma/d\Omega(\mu b/sr)$ 180 MeV	292 MeV
^{9}Be	296	Be	100	0.15±0.03	
^{12}C	227	C	99	0.40±0.05	
^{13}C	356	C	90	0.10±0.03	
^{16}O	880	H_2O	100	0.34±0.04	0.12±0.02
^{18}O	1040	H_2O	95	0.88±0.10	2.40±0.19
^{24}Mg	235	MgO	100	0.11±0.03	0.014±0.005
^{26}Mg	409	Mg	100		1.00±0.14
^{32}S	250	S	95	0.084±0.025	
^{209}Bi	534	Bi	100		0.46±0.15

ly, preserving the EPICS ray-tracing capabilities. A vacuum scattering chamber was constructed to fit between the magnet poles and was flexibly coupled to the channel as well as rigidly to the spectrometer, thus allowing the whole assembly to pivot with the spectrometer. The target position was maintained over the spectrometer pivot, at the upstream effective edge of the dipole field. Downstream of the target, the spectrometer center line was offset 10.16 cm to realign it with the extracted beam.

Some properties of the targets used in these experiments are listed in Table I. The ^{16,18}O targets were frozen water, enriched in the appropriate oxygen isotope. A typical DCX scattering spectrum (from ^{18}O) is shown in Fig. 3.

The extracted data are differential cross sections $d\sigma/d\Omega$ as functions of angle and/or energy. Seven-point angular distributions were measured over the range 5° to 33° in the laboratory. The excitation functions and A-dependence curves were measured at a laboratory angle of 5°. The data were normalized by comparing π^+p scattering yields to those predicted by π^+p phase-shift analysis.[16] The overall normalization is believed to be accurate to ±15%.

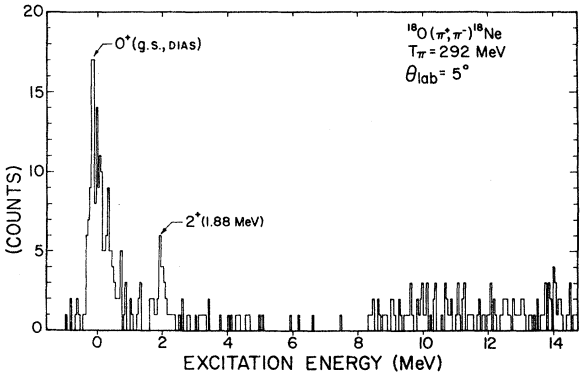

FIG. 3 Missing mass spectrum of $^{18}O(\pi^+,\pi^-)^{18}Ne$ at 292 MeV, 5°.

III. RESULTS

A. Excitation functions

$T=0,1$ isospin (isotope) pairs were chosen initially to study the isospin character of the reaction. The general features revealed are different from anything anticipated on the basis of previous measurements.[17]

The ^{16,18}O results are shown in Fig. 4. The ^{18}O (DIAS) measurements span the incident energy range $80 \leq T_m \leq 130$ MeV; the cross section shows

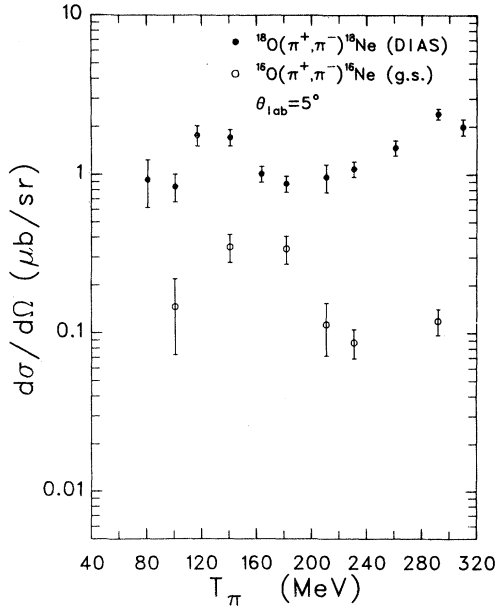

FIG. 4. Ground-state excitation functions at $5°_{lab}$ for (π^+,π^-) on ^{16,18}O.

a local maximum near 120 MeV which falls off by a factor of 2 as the energy approaches the resonance, but then increases by a factor of more than 2 as the energy increases beyond the resonance to ~300 MeV. The ^{16}O (g.s.) non-DIAS transition has a maximum near 160 MeV which drops sharply with decreasing energy, also falling steeply across the resonance (by a factor of ~4), leveling off above 200 MeV. The total range in ^{16,18}O cross sections is from ~2.4 μb/sr to ~120 nb/sr. The ^{24,26}Mg data are shown in Fig. 5; while there are fewer points, the pair of curves appear strikingly similar to the ^{16,18}O curves.

Near 160 MeV, the ratio $\sigma(^{18}\text{O})/\sigma(^{16}\text{O})$ is slightly larger than 3/1, but at 292 MeV it is ~20/1. The ^{24}Mg curve appears to peak at a lower energy than that of ^{16}O; the ratio $\sigma(^{26}\text{Mg})/\sigma(^{24}\text{Mg})$ is about 1/1 at 140 MeV and ~70/1 at 292 MeV. The overall shape of the two DIAS excitation functions differ in magnitude by nearly a constant factor, in the ratio $\sigma(^{18}\text{O})/\sigma(^{26}\text{Mg}) \simeq 3.2/1$. The non-DIAS shapes are more dissimilar in detail but have the same general features across the resonance.

DCX transitions were also observed to the 2_1^+ (1.89 MeV) first excited state of ^{18}Ne. Since the experimental runs were keyed to the observation of the ground-state transition, this excited state was only seen with poor statistics. The excitation function of this state is shown in Fig. 6. Its shape appears to be more similar to the ^{18}O DIAS curve than to the ^{16}O non-DIAS curve.

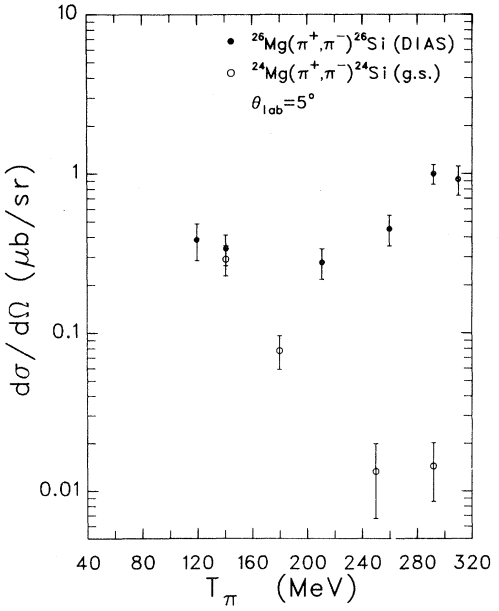

FIG. 5. Ground-state excitation functions at 5°$_{lab}$ for (π^+,π^-) on ^{24,26}Mg.

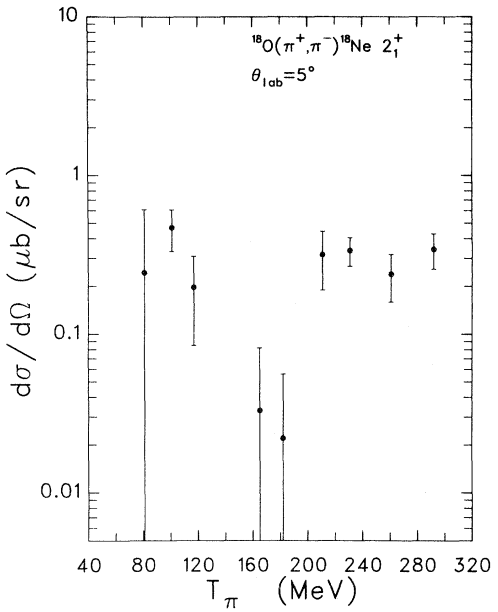

FIG. 6. Excitation function at 5°$_{lab}$ for ^{18}O$(\pi^+,\pi^-)^{18}$Ne (2_1^+, 1.89 MeV).

B. Angular distributions

At 164 MeV, the ^{18}O angular distribution shows a 5° cross section of ~1 μb/sr (Fig. 7) which falls to a minimum near 20° of about 40 nb/sr, climbing back to ~250 nb/sr at 33°, in good agreement with the previous measurement.[12] Figure 7 also shows the ^{18}O 292-MeV distribution, in which the position of the minimum (while less distinct) appears to have shifted outwards to near 25°.

The ^{26}Mg 292-MeV distribution is compared with the corresponding ^{18}O distribution in Fig. 8. The minimum appears to be in the range 26°–28°. Again, the ratio of magnitudes $\sigma(^{18}\text{O})/\sigma(^{26}\text{Mg})$ is nearly constant at forward angles.

A 164-MeV angular distribution was also measured for the 2_1^+ excited state of ^{18}Ne. As seen in Fig. 9, the shape appears to be consistent with a simple $\Delta l = 2$ transition.

C. *A* dependence

In the course of a series of mass measurements,[18] additional 180-MeV, 5° DCX cross sections were determined for ^{9}Be, ^{12,13}C, and ^{32}S. These cross sections, with those from the other targets at the same angle and energy, are listed in Table I and shown in Fig. 10. The data appear to fall into three groups, all decreasing in cross sec-

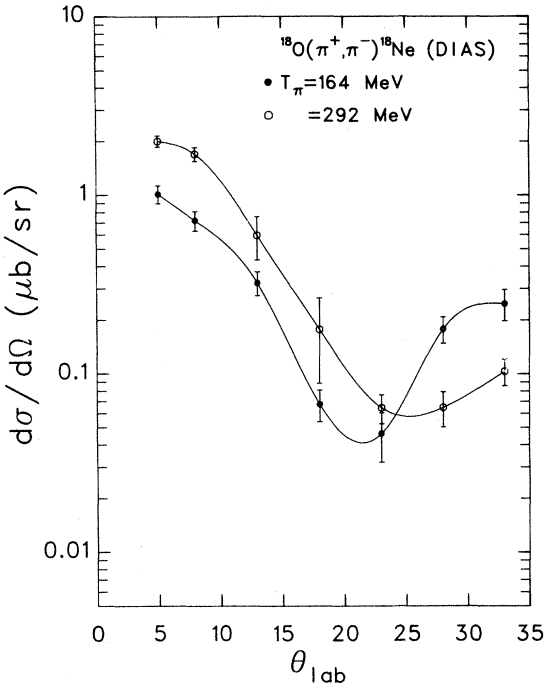

FIG. 7. Angular distributions at 164 and 292 MeV for $^{18}O(\pi^+,\pi^-)^{18}Ne$ DIAS. The lines are to indicate the minimum shift.

tion with increasing atomic number A. The $N=Z+2$ family have the highest cross sections and are roughly paralleled by the $N=Z$ (even-even) and $N=Z+1$ (even-odd) families in decreasing order.

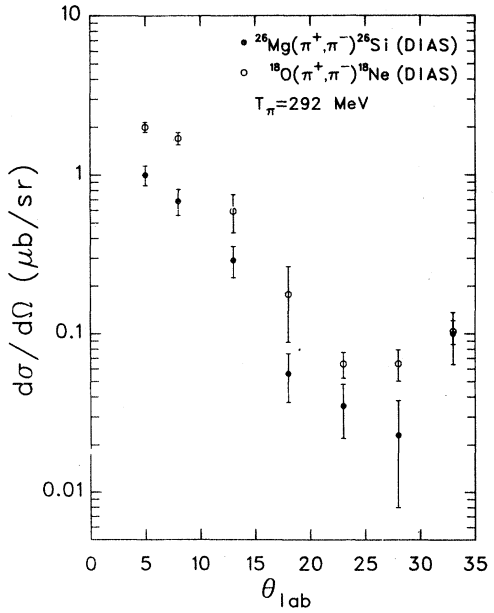

FIG. 8. Comparison, at 292 MeV, of the DIAS angular distributions from ^{18}O and ^{26}Mg.

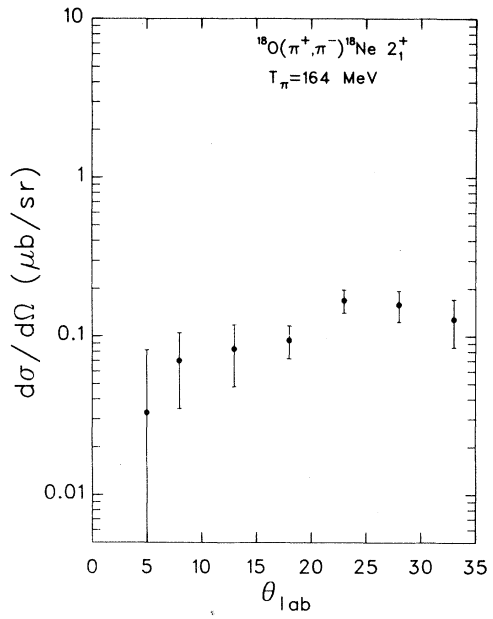

FIG. 9. Angular distributions at 164 MeV for $^{18}O(\pi^+,\pi^-)^{18}Ne$ (2_1^+, 1.89 MeV).

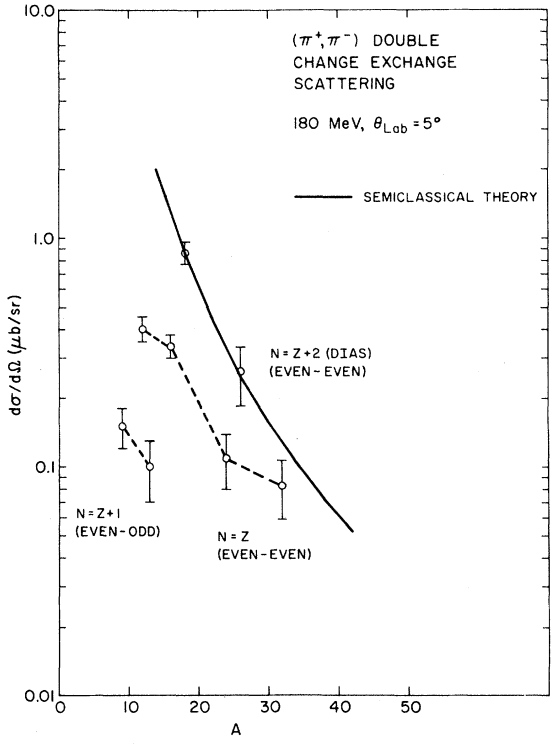

FIG. 10. Cross sections at 180 MeV, 5°, for (π^+,π^-) on nuclei of various A and N-Z. The solid curve through the $N=Z+2$ ($T=1$) nuclei is from the semiclassical treatment of Johnson, Ref. 20. The ^{26}Mg point is interpolated from the data in Fig. 5.

A DCX measurement was also made with a ^{209}Bi target at 292 MeV. Evidence was found for the ^{209}Bi$(\pi^+,\pi^-)^{209}$At DIAS transition.[19] For the purpose of comparison, a curve of the 292-MeV A dependence for all three DIAS transitions at 5° is shown in Fig. 11.

IV. DISCUSSION

A. Optical concepts

Many early considerations of DCX treated the reaction as two sequential single charge exchanges (SCX). A potential of the form

$$U = U_0 + U_1(\vec{t}\cdot\vec{\tau}) \tag{1}$$

was commonly assumed, where $\vec{t}$ and $\vec{\tau}$ are the pion and nuclear isospin operators, respectively. A recent Eikonal-model treatment by Johnson[20] based on this yields an angular and A dependence of the form

$$\sigma_{\mathrm{DCX}} \propto (N-Z)(N-Z-1)A^{-10/3}\left\{J_0(qR) - \frac{a}{R}[J_0(qr) - qRJ_1(qR)]\right\}^2 \tag{2}$$

the angular distribution is determined by the Bessel functions J_0 and J_1, with the cross section (for constant $N-Z$) scaling as $A^{-10/3}$. Such a formalism is only designed to consider $T \geq 1$ nuclei. The validity of Eq. (2) is limited to the region of p-wave dominance.

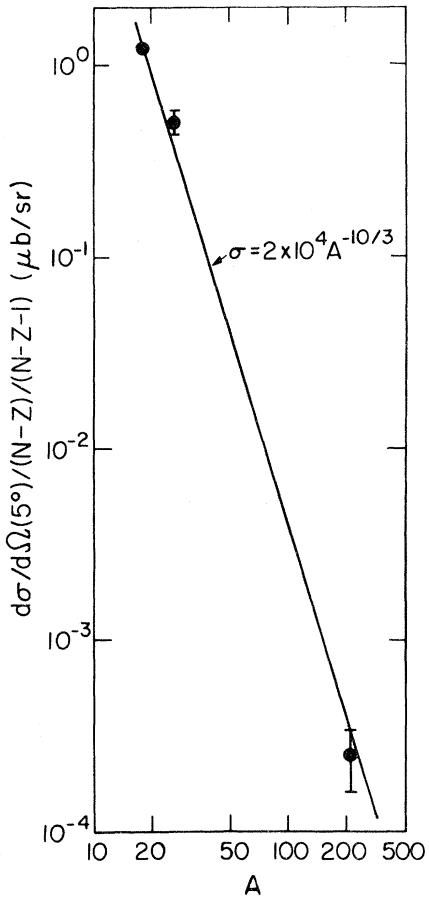

FIG. 11. Cross section at 292 MeV, 5°, for DIAS transitions from ^{18}O, ^{26}Mg, and ^{209}Bi. The solid line is due to Johnson, Ref. 20.

The π-nuclear diffractive model generally treats pion scattering near 180 MeV in terms of diffraction from a strong-absorption radius corresponding to the $\frac{1}{10}$ density point. As mentioned above, electron scattering[13] and pion elastic scattering[14] indicate an ^{18}O strong-absorption radius of $\sim$3.8 fm for which Eq. (2) predicts a minimum near 34°. The observed minimum near 21° would imply an ^{18}O nuclear size of $\sim$5.7 fm which is unphysically large.

Ignoring the assumption of p-wave dominance, for the moment, we observed that Eq. (2) correctly predicts the angular minimum at 292 MeV, for both ^{18}O and ^{26}Mg. Since the nucleus becomes more transparent to pions at this energy, the strong-absorption radius moves inward to the $\sim\frac{3}{10}$ density point.[21] A 25° minimum in the 292 MeV ^{18}O distribution yields a radius R in Eq. (2) of $\sim$3.1 fm in close agreement with the electron scattering value of $\sim$3.0 fm. Also, the 26°–28° minimum in the 292–MeV ^{26}Mg distribution yields the value $R \simeq 3.4$ fm, again in agreement with the electron scattering value of $\sim$3.5 fm.[22] This is surprising in that Eq. (2) is held to be valid only in the region of the (3,3)π-nucleon resonance, whereas at 292 MeV higher partial waves are known to be significant. This seems to indicate that an interference, in addition to that between J_0 and J_1, is present near 164 MeV and not at 292 MeV.

The factor $(N-Z)(N-Z-1)$ of Eq. (2), divided by two, is simply the number of possible valence-nucleon pairs. At the peak of the resonance, extrapolating the ^{26}Mg point from surrounding data, we note that an $A^{-10/3}$ curve can

be drawn through the two 5°, 180-MeV DIAS points, as seen in Fig. 10. Although Eq. (2) is not valid for $T<1$ nuclei, the data from these families are seen to roughly parallel the $T=1$ curve. This model, of course, gives no indication of a reason for such behavior.

An additional surprise is that Eq. (2) also seems to hold for the A dependence at 292 MeV. Figure 11 shows that an $(N-Z)(N-Z-1)A^{-10/3}$ curve nearly fits the three 5° DIAS points. Note, however, that the region $26<A<209$ is entirely unsupported by data. The sparseness of the data does not allow that Eq. (2) can be held to adequately represent the physics involved—especially when it seems to hold accurate in a region it was not meant for. There could be, for instance, additional $N-Z$ effects not accounted for by this semiclassical, first-order approach. If DCX is indeed sensitive to nuclear correlations it is not unreasonable that these higher-order effects could significantly alter the form of Eq. (2).

An approach to these higher-order effects which is currently being explored is the isobaric multiplet approach of Johnson and Siciliano.[23] In this model an optical potential of the form

$$U=-\vec{\nabla}\cdot[\xi(r)+\Delta\xi(r)]\vec{\nabla}+k^2[\bar{\xi}(r)+\Delta\bar{\xi}(r)] +\tfrac{1}{2}(p_1-1)\nabla^2\xi(r)+\tfrac{1}{2}(p_2-1)\nabla^2\Delta\xi(r) \quad (3)$$

is assumed, where $\bar{\xi}$ and ξ are s- and p-wave contributions to the first-order optical potential, and the $\Delta\xi$ are the higher-order contributions. The p_1 and p_2 terms correspond to kinematical corrections from the transformation from the π-nucleon center-of-mass to the π-nucleus center of mass.

The ξ are written, assuming isospin invariance,[24] as

$$\xi=\xi_0+\xi_1(\vec{t}\cdot\vec{\tau})$$

and

$$\Delta\xi=\Delta\xi_0+\Delta\xi_1(\vec{t}\cdot\vec{\tau})+\Delta\xi_2(\vec{t}\cdot\vec{\tau})^2\,, \quad (4)$$

where $\vec{t}$ and $\vec{\tau}$ are the pion and nucleon isospin operators, respectively. The $\Delta\xi$ introduce first-order terms quadratic in the nuclear density to the potential. While such terms have historically been found to have little effect on elastic scattering, we find they have a profound effect on charge-exchange calculations. Figure 12 demonstrates the capability of this approach to fit the anomalous DIAS angular distribution.

This formalism is being applied to $\pi^{\pm}$ elastic, (π^+,π^0) SCX, and (π^+,π^-) DCX scattering is an effort to relate them in a common phenomenology. The nuclear density dependence of the second-order terms is isoscalar (ρ^2), isovector ($\rho\Delta\rho$), and isotensor ($\Delta\rho^2$), where $\rho=\rho_n+\rho_p$ and $\Delta\rho=\rho_n-\rho_p$. Our method has been to calculate the strength of the first-order terms within the standard optical approach, and then to introduce the second-order strength to fit the DCX data, such strength being constrained within a predetermined theoretical range.[25] An indication of the effects of this treatment is shown in Fig. 12 in comparison with a typical first-order calculation.

This clearly demonstrates the usefulness, though not the validity, of such approaches. The validity can only be determined by testing this formalism with additional analog-DCX data, and by adapting it to handle inelastic and nonanalog charge exchange. The details of applying this formalism to the current data are being explored and will be presented in a forthcoming article.[26]

B. Interference effects

At 292 MeV, where $\sigma(T=1)/\sigma(T=0)$ is 20 or 70/1, very little ρ^2 strength is needed to fit the $T=1$ angular distributions. The possible need for a higher-order description of the DIAS seems to disappear when nonanalog (g.s.) transitions from the $T=0$ member of the $T=0,1$ pair become weak in comparison with those from the $T=1$ member.

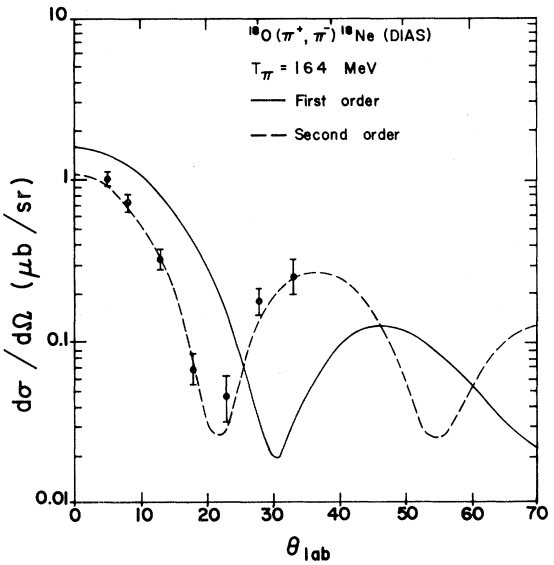

FIG. 12. Comparison of second-order optical approach of Johnson and Siciliano (dash) with typical first-order approach (solid).

This, together with the fact that nonanalog transitions can be large at certain energies (and unaccounted for in an isospin invariance picture) suggests an alternate picture of the DCX reaction mechanism.

We have previously reported[27] that the anomalous minimum from ^{18}O and the features of the ^{18}O excitation function may arise from the interference effects of two principal reaction amplitudes. This is apparent in the treatment of ^{18}O as $^{16}\mathrm{O} \otimes 2n$.

Some core configurations in ^{18}O are identical to configurations of ^{16}O.[28] Since the DCX cross sections from ^{16}O can be relatively strong, it is possible that similar contributions may be found from the core in the ^{18}O ground-state transition. Detailed calculations indicate that the relative strength of these components in ^{18}O as compared to ^{16}O may vary from 0.7 to 1.5. An estimate of unity for this ratio is sufficient for a qualitative discussion.

Modeling the ^{18}O DIAS core transitions on the observed ^{16}O data and combining this with a well known purely analog treatment[29] has yielded a good fit to the ^{18}O DIAS excitation function, where none previously existed (Fig. 13). This model might also account for the anomalous angular distribution. Where the core amplitude is strongest, near 160 MeV, it may interfere strongly with the pure analog amplitude and shift the resulting minimum.

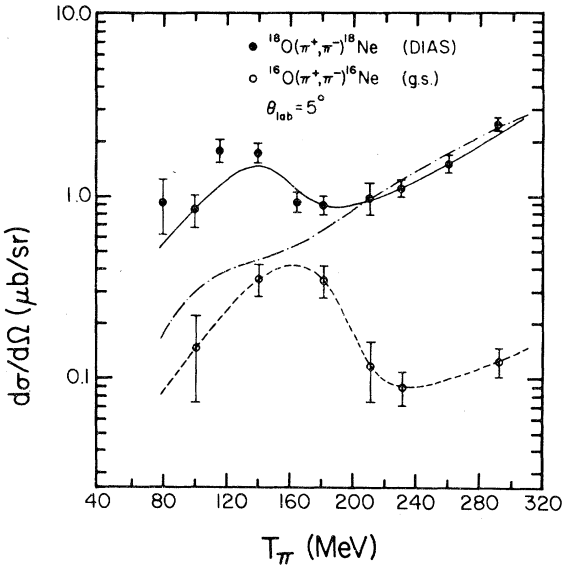

FIG. 13. The two-amplitude model. The dash-dot line is the square of the DIAS amplitude, and the dashed line is the square of the non-DIAS amplitude. The solid line is the squared sum of the amplitudes, added with a smoothly-varying energy-dependent phase.

V. CONCLUSIONS

The systematic behavior of the excitation functions and angular distributions of the $T=0,1$ isotope pairs revealed in this work confirm the expected strong dependence of DCX on isospin, but also suggest that the process is dominated more by the reaction mechanism than by nuclear structure effects. Such a dominance is also suggested by the limited data on the A dependence. The nondiffractive position of the minimum in the ^{18}O angular distribution at 164 MeV and the more diffractive angular distributions of ^{18}O and ^{26}Mg at 292 MeV suggest a complex reaction mechanism with a strong energy dependence, possibly consisting of several amplitudes. One approach to this problem, which is currently being pursued with some success, involves the use of a second-order optical potential with isovector and isotensor terms, to which SCX and DCX are much more sensitive than elastic scattering. Another possibility, suggested by the large nonanalog cross sections, is a model involving both analog and nonanalog amplitudes for the $T=1$ nuclei. Because of the current phenomenological nature of these two approaches, they may not be necessarily independent.

These ideas are based on a fairly limited data set, with three angular distributions for $T=1$ nuclei, only one of which is anomalous, some small-angle excitation functions, and information on the A dependence for a few nuclei. To pursue this work further more data are needed, including angular distributions for $T=0$ nuclei, more angular distributions for $T=1$ nuclei, and more information on the A and $(A-Z)$ dependence at the energies where the nonanalog transitions are strong and where they are weak. We anticipate that some of these data will be forthcoming in the near future, and we believe that they will cast new light on this intriguing and surprising process and ultimately lead to a further understanding of nuclear structure.

ACKNOWLEDGMENTS

The authors extend their thanks to the LAMPF MP-10 staff for enthusiastic support of the DCX design and EPICS modification effort. We are

grateful to the University of Chicago for the loan of the "Chicago-C" magnet and to R.L. Burman and K.K. Seth for the loan of the ^{26}Mg. We especially thank H.T. Fortune for many enlightening and fruitful discussions on interference effects. This work was supported by the U.S. Department of Energy, the Robert A. Welch Foundation, and the Associated Western Universities.

---

*Present address: New Mexico State University, Las Cruces, New Mexico 88003.
†Present address: University of Minnesota, Minneapolis, Minnesota 55455.
‡Present address: New Mexico State University, Las Cruces, New Mexico 88003.
§Present address: University of South Carolina, Columbia, South Carolina 29208.
||Present address: Stanford University, Stanford, California 94025.

[1]T. Ericson, CERN Report No. 63-28, 1963 p. 68 (unpublished); A. de-Shalit, S. D. Drell, and H. J. Lipkin, as reported in S. Barshay and G. E. Brown, Phys. Lett. 16, 165 (1965), and by R. G. Parsons in Ref. 3; A. K. Kerman and R. K. Logan, Argonne National Laboratory, ANL Report No. ANL 68-48, 1964 (unpublished).
[2]Ericson in Ref. 1.
[3]R. G. Parsons, J. S. Trefil, and S. D. Drell, Phys. Rev. 138, B847 (1965).
[4]W. B. Kaufmann, J. C. Jackson, and W. R. Gibbs, Phys. Rev. C 9, 1340 (1974).
[5]L. C. Liu and V. Franco, Phys. Rev. C 11, 760 (1975).
[6]G. A. Miller and J. E. Spencer, Phys. Lett. 53B, 329 (1974); Ann. Phys. (N.Y.) 100, (1976); E. Rost and G. Edwards, Phys. Lett. 37B, 247 (1971).
[7]S. Barshay and G. E. Brown in Ref. 1.
[8]L. Gilly, M. Jean, R. Meunier, M. Spighel, J. P. Stroot, P. Dutiel, and A. Rode, Phys. Lett. 11, 224 (1964).
[9]C. J. Cook, M. E. Nordberg, and R. L. Burman, Phys. Rev. 174, 1374 (1968).
[10]R. L. Burman, M. P. Baker, M. D. Cooper, R. H. Heffner, D. M. Lee, R. P. Redwine, J. E. Spencer, T. Marks, D. J. Malbrough, B. M. Preedom, R. J. Holt, and B. Zeidman, Phys. Rev. C 17, 1774 (1978).
[11]C. Perrin, J. P. Albanese, R. Corfu, J. P. Egger, P. Gretillat, C. Lunke, J. Piffaretti, E. Schwarz, J. Jansen, and B. M. Preedom, Phys. Lett. 69B, 301 (1977).
[12]K. K. Seth, S. Iverson, H. Nann, M. Kaletka, J. Hird, and H. A. Thiessen, Phys. Rev. Lett. 43, 1574 (1979); Los Alamos Scientific Laboratory Report No. LA-7892-C, 1979, p. 201 (unpublished).
[13]R. P. Singhal, J. P. Moreira, and H. S. Caplan, Phys. Rev. Lett. 24, 73 (1970).
[14]S. G. Iverson, Ph. D. dissertation, Northwestern University, 1979 (unpublished); Los Alamos Scientific Laboratory Report No. LA-7828-I, 1979 (unpublished).
[15]H. A. Thiessen *et al.*, Los Alamos Scientific Laboratory Report No. LA-4534-MS (unpublished); H. A. Thiessen, J. C. Kallne, J. F. Amann, R. J. Peterson, S. J. Greene, S. L. Verbeck, G. R. Burleson, S. G. Iverson, A. W. Obst, K. K. Seth, C. F. Moore, J. E. Bolger, W. J. Braithwaite, D. C. Slater, and C. L. Morris, Los Alamos Scientific Laboratory Report No. LA-6663-MS, 1977 (unpublished).
[16]G. Rowe, M. Salomon, and R. H. Landau, Phys. Rev. C 18, 584 (1978).
[17]G. R. Burleson Los Alamos Scientific Laboratory, Report No. LA-8303-C, 1980 p. 195 (unpublished).
[18]G. R. Burleson, G. S. Blanpied, G. H. Daw, A. J. Viescas, C. L. Morris, H. A. Thiessen, S. J. Greene, W. J. Braithwaite, W. B. Cottingame, D. B. Holtkamp, I. B. Moore, and C. F. Moore, Phys. Rev. C 22, 1180 (1980).
[19]C. L. Morris, H. A. Thiessen, W. J. Braithwaite, W. B. Cottingame, S. J. Greene, D. B. Holtkamp, I. B. Moore, C. F. Moore, G. R. Burleson, G. S. Blanpied, G. H. Daw, and A. J. Viescas, Phys. Rev. Lett. 45, 1233 (1980).
[20]M. B. Johnson, Phys. Rev. C 22, 192 (1980); Los Alamos Scientific Laboratory Report No. LA-7892-C, 1979 p. 343 (unpublished).
[21]M. B. Johnson and H. A. Bethe, Common. Nucl. Part. Phys. 8, 75 (1978); J. F. Germond and C. Wilkin, Nucl. Phys. A237, 477 (1975); C. Wilkin in Proceedings of the Second International Topical Conference on Meson-Nuclear Physics, Houston, Texas, 1979 p. 537 (unpublished); C. L. Morris, private communication.
[22]C. W. De Jager, H. De Vries, and C. De Vries, At. Data Nucl. Data Tables 14, 479 (1974).
[23]M. B. Johnson and E. R. Siciliano (unpublished).
[24]M. B. Johnson and E. R. Siciliano (unpublished).
[25]E. R. Siciliano and M. B. Johnson, Bull. Am. Phys. Soc. (in press).
[26]S. J. Greene, M. B. Johnson, and E. R. Siciliano (unpublished).
[27]S. J. Greene, D. B. Holtkamp, W. B. Cottingame, C. Fred Moore, G. R. Burleson, C. L. Morris, H. A. Thiessen, and H. T. Fortune, Phys. Rev. C (to be published).
[28]T.-S. Lee, D. Kurath, and B. Zeidman, Phys. Rev. Lett. 39, 1307 (1977).
[29]G. A. Miller, Bull. Am. Phys. Soc. 25, 731 (1980).
[30]Liu Xianhui, Wu Zongen, Huang Zhaohui, and Li Yangguo, Sci. Sin. 24, 789 (1981).